

Electrical and optical properties of $\text{Cu}_2\text{ZnSnS}_4$ thin films prepared by rf magnetron sputtering process

Jae-Seung Seol^{a,*}, Sang-Yul Lee^a, Jae-Choon Lee^a,
Hyo-Duk Nam^b, Kyoo-Ho Kim^a

^a*School of Metallurgical and Materials Engineering, Yeungnam University, Kyongsan, Yeungnam 712-749, South Korea*

^b*School of Electrical and Electronic Engineering, Yeungnam University, Kyongsan 712-749, South Korea*

Abstract

$\text{Cu}_2\text{ZnSnS}_4$ thin films were deposited on corning 7059 glass substrates without substrates heating by rf magnetron sputtering. The Cu/(Zn + Sn) ratio of the thin film sputtered at 75 W was close to the stoichiometry of $\text{Cu}_2\text{ZnSnS}_4$. However, the S/(Cu + Zn + Sn) ratio was less than the stoichiometry. The as-deposited films were amorphous and annealed in the atmosphere of Ar + S₂ (g). The annealed (1 1 2), (2 0 0), (2 2 0), (3 1 2) planes were conformed to all the reflection of a kesterite structure. A preferred (1 1 2) orientation was observed with the increase of the annealing temperature. The optical absorption coefficient of the thin film was about $1.0 \times 10^4 \text{ cm}^{-1}$. The optical band energy was derived to be 1.51 eV. The optical absorption coefficient of the sputtered $\text{Cu}_2\text{ZnSnS}_4$ thin films was less than that of CuInS_2 thin film, however, the band gap energy was more appropriate for photovoltaic materials. © 2002 Elsevier Science B.V. All rights reserved.

1. Introduction

CuInS_2 (CIS) is the chalcopyrite-type semiconductors which has a direct energy band gap ($E_g = 1.08 \text{ eV}$) and a large optical absorption coefficient. However, we know In in this system is expensive element for commercializing. In the study, we synthesized $\text{Cu}_2\text{ZnSnS}_4$ (CZTS) compounds on the glasses by rf magnetron sputtering for reducing the cost of CIS solar cell. CZTS compound was derived by replacing the half of indium (In) atoms with zinc (Zn) atoms and the other half with

*Corresponding author.

tin (Sn) atoms in the chalcopyrite-type lattice of CIS. It is known that CZTS is one of the potential photovoltaic materials for use as low-cost thin films solar cells due to appropriate band gap of 1.4–1.5 eV, as well as a good absorption coefficient. However, the study on CZTS cells has not been studied for several years due to the lack of the detailed understanding of the parameters governing the performance and low-efficiency. In this study, we investigated the physical, electrical and optical properties of these thin films for a solar cell application.

2. Experimental

CZTS thin films were deposited on corning 7059 glass substrates without substrates heating by rf magnetron sputtering. The target, composed of finely mixed Cu_2S , ZnS and SnS_2 was cold-pressed at 250 MPa. After a deposition, thin films were annealed in atmosphere of $\text{Ar} + \text{S}_2(\text{g})$ at 250–400°C. ($\Phi 30$ mm quartz tube, 800 sccm), the composition of thin films was determined by energy dispersive spectroscopy (Fisons, dispersive spectroscopy, Fisons, Kevex Super Dry) for the chemical composition and X-ray diffractometer (XRD, Phillips) with a Cu K_α radiation for the phase identification and crystallographic structure. The surface morphology of the thin films was observed by SEM (Hitachi S-4100). The Electrical resistance of the thin films was measured using a four-point probe (CMT-SR1000N, Changmin Co.) and the optical transmittance of the thin films was measured with an UV-VIS-NIR Spectrophotometer (CARY 5G, Varian) in the wavelength range of 300–2500 nm. The band gap energy was derived from the plot of $\alpha^2 - h\nu$, where, α is the absorption coefficient. $h\nu$ is the photon energy (Table 1).

3. Results and discussions

In the case of sputtering target with $\text{Cu}_2\text{S}:\text{ZnS}:\text{SnS}_2 = 1:1:1$, the Zn and Sn contents of the thin films increased but the Cu content decreased. Thus we changed the atomic ratio of the sputtering target with $\text{Cu}_2\text{S}:\text{ZnS}:\text{SnS}_2 = 2:1.5:1$ to obtain the

Table 1
Experimental conditions

Parameters	Conditions
Sputter source	Radio frequency (13.56 MHz)
Discharge	Ar (2 sccm)
Purging method	Ar (10 sccm)
Working pressure	25 mTorr
rf Power	50–150 W
Sputtering time	120 min
Substrate temperature	Room temperature
Substrate	Corning 7059 glass

stoichiometric ratio of CZTS thin films. Fig. 1 shows atomic ratio in the CZTS thin films deposited on corning 7059 glass substrates at room temperature as the function of rf power.

The atomic ratio of the thin films obtained at rf power between 50 and 100 W was appropriate. However, at above 100 W of rf power, the Cu content of CZTS thin films was rapidly decreased, but the Sn content was significantly increased. It is believed that the abrupt change of the Cu and Sn contents with the rf power depend upon the plasma density.

Fig. 2 shows the atomic percent of CZTS thin films deposited at the 75 W of rf power for 2 h annealed at 250–400°C for 1 h in atmosphere of Ar + S₂ (g) using tube furnace. The as-deposited CZTS thin films were stoichiometric, except sulfur. However, we obtain close to stoichiometric composition of CZTS thin films by annealing at above 200°C in sulfur vapor atmosphere.

Fig. 3 shows the XRD patterns of the thin films annealed in atmosphere of Ar + S₂ (g). In Fig. 3, the crystallization of the thin films occurred when it was annealed at above 250°C. The major diffraction peaks of the CZTS thin films were corresponded to (1 1 2), (2 0 0), and (2 2 0), (3 1 2) planes.

The crystal structure of the thin films was identified as the kesterite structure. As annealing temperature increased, the intensity of the (1 1 2) preferred orientation was stronger. This result expected the improvement of conversion efficiency, reported by Yamacuchi.

Fig. 4 shows that the surface morphology of the CZTS thin films annealed at 250–400°C. The degree of the crystallinity of CZTS thin films increased with the increase of annealing temperature.

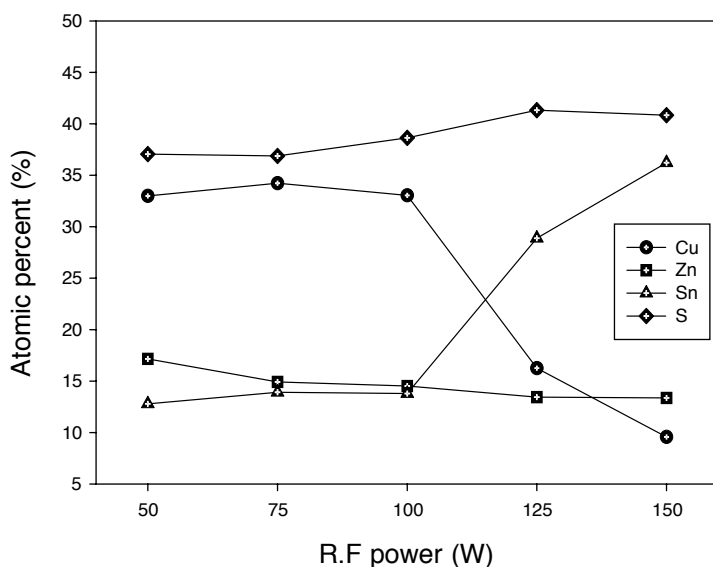


Fig. 1. Atomic percent of the CZTS thin films as a function of rf power (Cu₂S:ZnS:SnS₂=2:1.5:1).

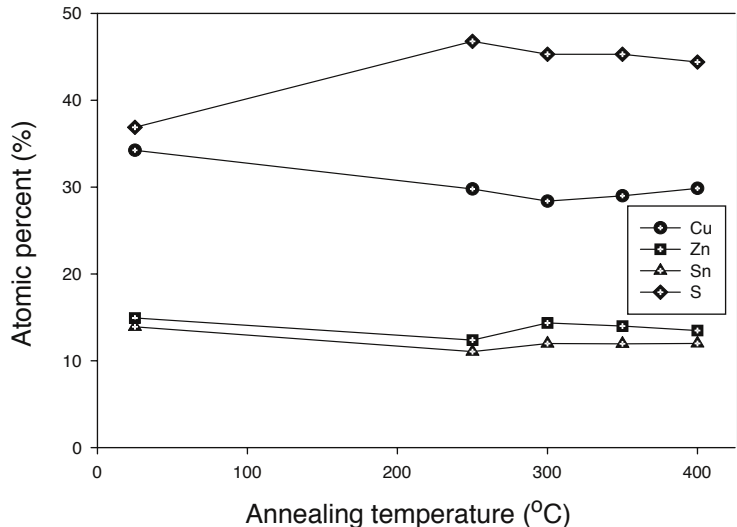


Fig. 2. Atomic percent of the CZTS thin films as the function of annealing temperature ($\text{Cu}_2\text{S}:\text{ZnS}:\text{SnS}_2 = 2:1.5:1$).

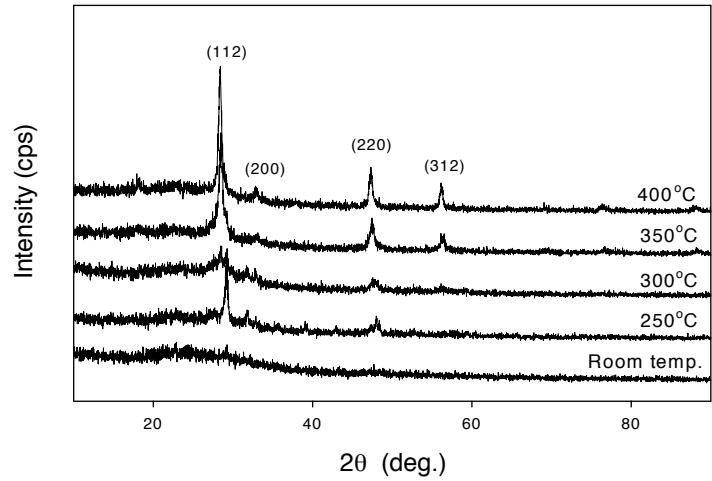


Fig. 3. XRD patterns of CZTS thin films deposited on corning 7059 glass substrates at 75 W of rf power as the function of annealing temperature.

The sheet resistance was decreased rapidly with the increase of annealing temperature in Fig. 5. This result can perhaps be explained by the degree of crystallization as shown in XRD results (Fig. 3). The sheet resistance of thin films annealed at 400 °C in atmosphere of $\text{Ar} + \text{S}_2$ (g) was below $0.47 \Omega \text{ cm}$.

Fig. 6 shows the optical transmittance of CZTS thin films deposited with 75 W of rf power and annealed at 400 °C, which was measured in the range 400–2500 nm

Fig. 4. Surface morphology of the CZTS thin films as the function of annealing temperature (a) as-deposited (b) 300°C (c) 350°C (d) 400°C.

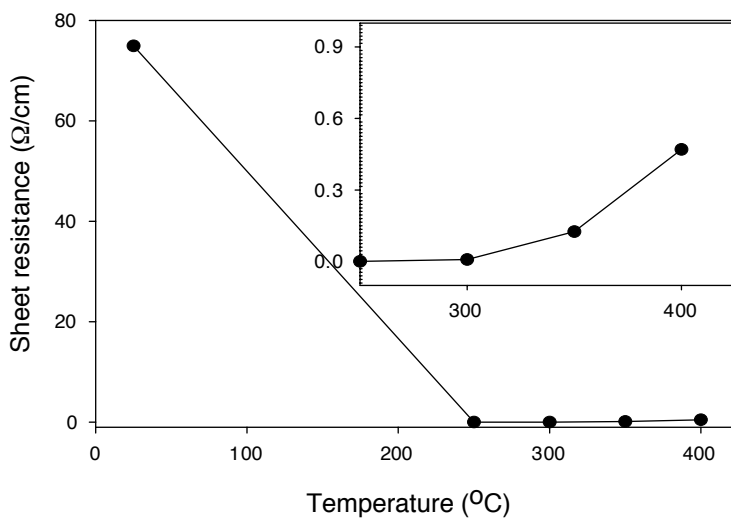


Fig. 5. Sheet resistance in the CZTS thin films deposited on corning 7059 glass substrate at 75 W of rf power as the function of annealing temperature.

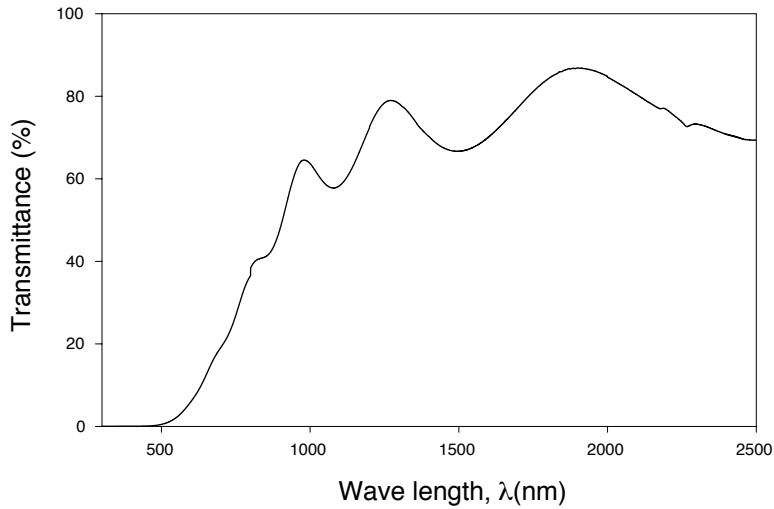


Fig. 6. Optical transmittance of CZTS thin films deposited with 75 W of rf power and annealed at 400°C.

using the UV-VIS-NIR spectrophotometer. When used in a solar cell, the thin films can absorb the photon energy consisting of the visible and infrared rays. At a long wavelength range, the transmitted light spectrum with wave curve results in the interference.

The absorption coefficient (α) and the refractive index (n_f) were derived from the optical transmittance.

$$\alpha = -t^{-1} \ln \frac{-(1-R)^2 + \sqrt{(1-R)^4 + 4T^2R^2}}{2T^2R^2}, \quad (1)$$

where t is the thickness of the thin films, R is the reflexivity of the thin films, T is the transmittance of CZTS thin films and n_f is the refractive index of thin film. The refractive index (n_f) of CZTS thin films using an interference fringe was 2.07.

$$R = \left(\frac{n_f + 1}{n_f - 1} \right)^2, \quad n_f = (4t)^{-1} \left| \frac{\lambda_{\max} \times \lambda_{\min}}{\lambda_{\max} - \lambda_{\min}} \right|.$$

Fig. 7 shows the optical absorption coefficient of the CZTS thin films deposited with 75 W of rf power and annealed at 400°C. The absorption coefficient (α) of the CZTS thin films was lower than $1 \times 10^4 \text{ cm}^{-1}$, which reported by Ito and Nakazawa from measuring a CIS thin films solar cell.

Fig. 8 shows the energy band gap of the CZTS thin films deposited with 75 W of rf power and annealing temperature of 400°C. The energy band gap of the thin films was 1.51 eV. This value appears to be an appropriate energy band gap for a solar cell.

The optical absorption coefficient at about 1.3 eV of Fig. 7 and α^2 at about 1.55 eV of Fig. 8 were shifted because of the detector changeover as a wavelength scale in the other UV-VIR-NIR spectrophotometer.

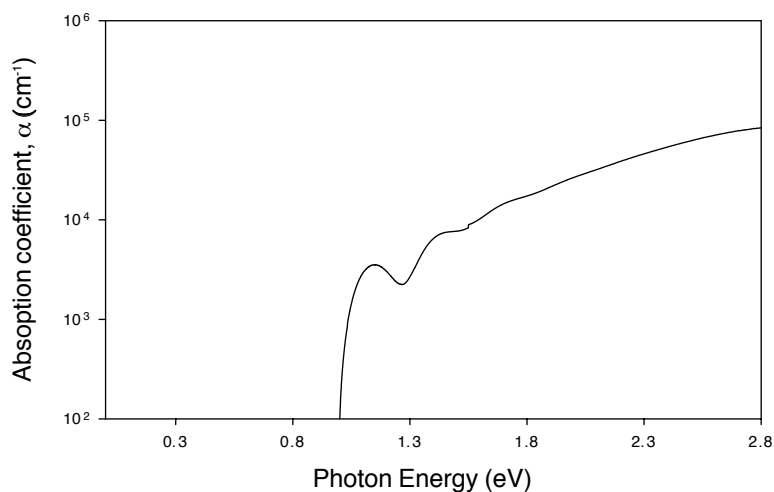


Fig. 7. Optical absorption coefficient of CZTS thin films deposited with 75 W of rf power and annealed at 400°C.

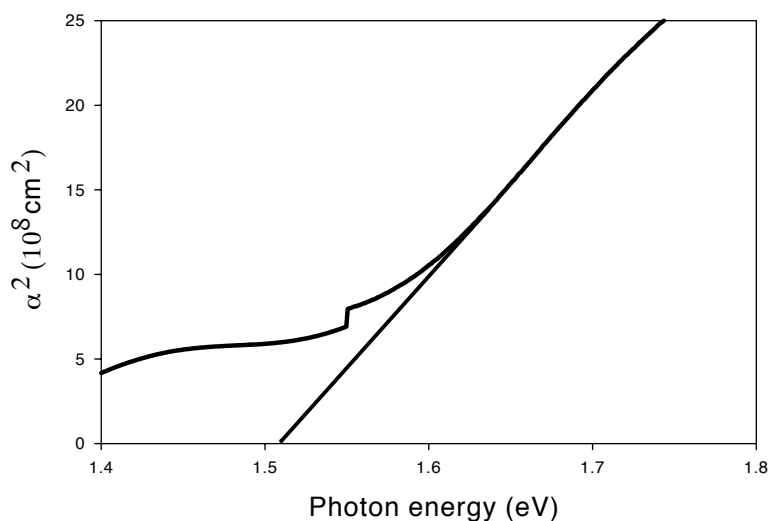


Fig. 8. Energy band gap of CZTS thin films deposited with 75 W of rf power and annealed at 400°C.

4. Conclusion

We obtained that as-deposited films without substrate heating were amorphous, while all annealed films showed the distinct diffraction peaks of CZTS, which were identified to the (1 1 2), (2 0 0) and (2 2 0), (3 1 2) planes, respectively. The peak of a preferred (1 1 2) orientation was stronger than that of diffraction peaks of CIS cells with increasing the annealing temperature.

With the increase of annealing temperature, the crystallinity of CZTS thin films was improved, and the sheet resistance decreased rapidly. The sheet resistance of the thin films annealed at 400°C in atmosphere of Ar + S₂ (g) were below 0.47 Ω cm. In the CZTS thin film deposited with 75 W of rf power and annealed at 400°C, the refractive index (n_f) was 2.07, the absorption coefficient (α) was about $1.0 \times 10^4 \text{ cm}^{-1}$ which is less than that of CIS thin films, and the band gap was about 1.51 eV which was better than that of CIS cells for solar cell applications.

5. For further reading

The following references may also be of interest to the reader: [1–19].

References

- [1] M.A. Green, J. Zhee, *Proc IEEE Electron Dev. Lett.* 13 (6) (1992) 317–318.
- [2] B.R. Pamplin, T. Kiyosawa, K. Masumoto, *Prog. Cryst. Growth Charac.* 1 (1) (1979) 331.
- [3] Yamamoto, M. Yamaguchi, *Appl. Phys. Lett.* 44(6) (1984) 611–613.
- [4] C. Rincon, C. Beilabarba, J. Gonzalez, *Solar Cells* 16 (1986) 335.
- [5] H. Takakura, *Jpn. J. Appl. Phys.* 31 (1992) 2394.
- [6] K. Zwejbel, S. Harin, *Proceedings of the 23rd IEEE Photovoltaic Specialists Conference*, 1993, pp. 379–388.
- [7] T. Tanaka, Y. Demizu, Yamaguchi, *Jpn. J. Appl. Phys.* 35 (1996) 2779–2781.
- [8] J.W. Park, G.Y. Chung, H.B. Im, *Thin Solid Films* 245 (1994) 174–179.
- [9] K.W. Mitchell, C. Eberspacher, J. Ermer, *Proceedings of the 20th IEEE Photovoltaic Specialists Conference*, 1989, p. 1384.
- [10] R.H. Mauch, J. Hedstrom, D. Lincot, *Proceedings of the 20th IEEE Photovoltaic Specialists Conference*, Vol. 2, 1991, p. 898.
- [11] S.R. Hall, J.T. Szymariski, J.M. Stewart, *Can. Miner.* 16 (1978) 131.
- [12] Hironori Katagiri, Naoya Ishigaki, Masato Nishimura, *The Institute Electronics Information and Communication Engineers*, 1997, p. 53.
- [13] D.S. Lickerby, A. Matthews, *Advanced Surface Coatings*, Blackie & Son Ltd. Publishers, 1991, Chapter 5.
- [14] R. Nitsche, D.F. Sargent, P. Walter, *J. Cryst. Growth* 1 (1) (1969) 52.
- [15] T.M. Friedlmeier, N. Wieser, T. Walter, H. Dittrich, H.W. Schock, *Proceedings of the 14th PVSEC*, 1997, p. 254.
- [16] K. Ito, T. Nakazawa, *Jpn. J. Appl. Phys.* 27 (1988) 2094.
- [17] N. Nakayama, K. Ito *Appl. Surf. Sci.* 92 (1996) 171.
- [18] Theresa Magorian Friedlmeier, Herbert Dittrich and Hans-Werner Schock, *Inst. Phys. Conf. Ser.* 152, Section B, 1997, p. 345.
- [19] T. Yamaguchi, et al., *J. Appl. Phys.* 69 (1991) 7714.